A Full Wave Analysis of Microstrips by the Boundary Element Method

Shih-Yuan Lin and Chin C. Lee, *Senior Member, IEEE*

***Abstract*—In this paper, the boundary element method (BEM) is formulated to carry out a full wave analysis of microstrip lines. Numerical results for frequency dependence of effective dielectric constant and calculated longitudinal and transverse current distributions are presented. Fundamental and higher order modes supported by the microstrip are identified and characterized. Compared with other techniques, the present method requires less memory size without requiring intricate mathematical skills because of the inherent characterization of BEM in needing only to discretize the boundary of the structure. Through our simulation, it shows that this method can reduce memory size as well as the computation time. Numerical results also show good agreement with available data in literature.**

I. Introduction

In modern microwave integrated circuits, the microstrip line has become one of the most important and fundamental components. In earliest publications, microwave propagation was treated in the quasi-TEM mode [1]–[4]. In quasi-TEM approximation, the Poisson's equation rather than the Helmholtz equation is solved. Thus, the resultant parameters, such as effective dielectric constant, are independent of frequency. The quasi-TEM approximation was subsequently used in most publications [5], [6]. This approximation is valid only when the cross-section geometry of microstrip structure is much smaller than the wavelength of the propagation wave. Beyond this constraint, microstrip line is dispersive and departs from the behavior predicted by quasi-TEM analysis. Since a microstrip line contains two different dielectric media, all of the propagation modes are hybrid. Thus, it is necessary to use full-wave analysis to find the properties of propagation modes. Various methods have been developed to examine the dispersion characteristics. Typical methods are Green's function [7], finite difference [8] and [9], spectral-domain [10]–[12], finite element [13] and [14], tangential vector finite elements [15], and variational finite elements [16]. Recently, the boundary element method (BEM) [17] has also been used in the analysis of waveguide problems [18]–[20], and magnetostatic waves [21]. However, in analyzing microstrip line, BEM was used only in quasi-TEM approximation [22].

In this paper, we perform a full wave analysis of microstrip using the BEM. The effective dielectric constants for fundamental and higher order modes are calculated. Longitudinal and transverse current distributions are obtained by way of the field solution. Besides the regular microstrip line, the method formulated is also employed to analyze coupled microstrip lines. The results indicate significant difference in the propagation velocity between the even- and odd-modes. In BEM, since the boundary integral is performed merely along the contour, the required memory size and computation time are considerably reduced. For the chosen structures that were studied by others, our calculated results agree quite well with the reported data.

Manuscript received February 13, 1995; revised July 22, 1996.

The authors are with the Department of Electrical and Computer Engineering, University of California, 2226 Engineering Gateway, Irvine, CA 92697 USA.

Publisher Item Identifier S 0018-9480(96)07914-8.

II. Boundary Element Method for the Helmholtz Equation

In this method, the Helmholtz equation is converted to an integral equation by way of the Green's second identity [23]

$$\iint (g\nabla^2\phi - \phi\nabla^2 g)\, dS = \oint \left(g\frac{\partial\phi}{\partial n} - \phi\frac{\partial g}{\partial n}\right) d\Gamma \quad (1)$$

where the region S is surrounded by the contour Γ shown in Fig. 1. Inside the region S, ϕ, and g satisfy the Helmholtz and point source equations, respectively, i.e.,

$$\begin{aligned}(\nabla^2 + k_t^2)\phi &= 0\\ (\nabla^2 + k_t^2)g &= -\delta(\vec{r} - \vec{r}')\end{aligned} \quad (2)$$

where $\delta(\cdot)$ is the Dirac Delta function and g is the two-dimensional (2-D) Green's function that can be chosen as $[(-j)/4]H_0^{(2)}(k_t|\vec{r} - \vec{r}'|)$ for the propagation wave ($k_t^2 > 0$), and $(1/2\pi)K_0(\bar{k}_t|\vec{r} - \vec{r}'|)$ for the evanescent wave ($k_t^2 = -\bar{k}_t^2 < 0$). Here $H_0^{(2)}$ is the zeroth order Hankel function of the second kind and K_o is the modified Bessel function [23]. Substituting (2) into (1) results in

$$C_j\phi(p_j) = \oint g_j \frac{\partial\phi}{\partial n}\, d\Gamma - \oint \phi \left(\frac{\partial g}{\partial n}\right)_j d\Gamma \quad (3)$$

where C_j is obtained by the Cauchy principal value integration and is given by [18] and [21]

$$C_j = \begin{cases} 0, & p_j \notin \Gamma + S \\ 1, & p_j \in S \\ \dfrac{\theta}{2\pi}, & p_j \in \Gamma \end{cases}$$

where θ is the angle spanned by contour Γ at point p_j, as indicated in Fig. 1. Upon discretization on Γ, (3) is converted into

$$C_j\phi_j = \sum_{k=1}^{N} \int g_j \frac{\partial\phi}{\partial n}\, d\Gamma_k - \sum_{k=1}^{N} \int \phi \left(\frac{\partial g}{\partial n}\right)_j d\Gamma_k \quad (4)$$

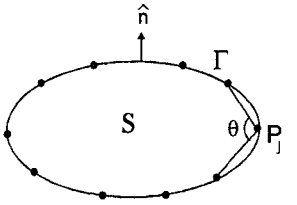

Fig. 1. Two-dimensional model for BEM and spanning angle at point P_j on boundary Γ.

where $\phi_j = \phi(p_j)$. Through linear interpolation, ϕ and $(\partial\phi)/(\partial n)$ within the kth segment Γ_k between points p_k and p_{k+l} can be evaluated as

$$\begin{cases} \phi(\vec{r}) = w_1\phi_k + w_2\phi_{k+1} \\ \dfrac{\partial\phi}{\partial n}(\vec{r}) = w_1\left(\dfrac{\partial\phi}{\partial n}\right)_k + w_2\left(\dfrac{\partial\phi}{\partial n}\right)_{k+1} \end{cases} \tag{5}$$

where w_1, and w_2 are linear interpolation factors. Substituting (5) into (4) yields

$$\sum_{k=1}^{N} A_{jk}\phi_k + \sum_{k=1}^{N} B_{jk}\left(\frac{\partial\phi}{\partial n}\right)_k = 0 \tag{6}$$

where

$$\begin{cases} A_{jk} = C_j\delta_{jk} + \displaystyle\int \left(\frac{\partial g}{\partial n}\right)_j w_1\, d\Gamma_k \\ \qquad\quad + \displaystyle\int \left(\frac{\partial g}{\partial n}\right)_j w_2\, d\Gamma_{k-1} \\ B_{jk} = -\displaystyle\int g_j w_1\, d\Gamma_k - \int g_j w_2\, d\Gamma_{k-1} \end{cases}.$$

III. Formulation for the Microstrip Line Problem

Fig. 2 depicts the cross section of an open microstrip line with infinite extent in both x- and z-direction and negligible strip thickness. The dielectric substrate is assumed lossless, homogeneous and isotropic. Relative permittivity and permeability of the substrate are ε_r and μ_r, respectively. μ_r is assumed to be one in this paper. Both the strip and ground plane are perfect conductor. Propagation with $e^{-j\beta z}$ dependence in the z direction and time variance of e^{jwt} are assumed. Since the four transverse field components E_x, E_y, H_x, and H_y, can be expressed in terms of E_z, and H_z, in both the dielectric and free space regions, it is sufficient to solve the pair of Helmholtz equations given as

$$\begin{cases} \nabla_t^2 E_z + k_t^2 E_z = 0 \\ \nabla_t^2 H_z + k_t^2 H_z = 0 \end{cases} \tag{7}$$

where

$$\nabla_t^2 = \frac{\partial^2}{\partial x^2} + \frac{\partial^2}{\partial y^2}$$

and

$$k_t^2 = \begin{cases} k_a^2 = \omega^2\varepsilon_0\mu_0 - \beta^2, & y > h \\ k_d^2 = \omega^2\varepsilon_0\varepsilon_r\mu_0 - \beta^2, & 0 < y < h \end{cases}. \tag{8}$$

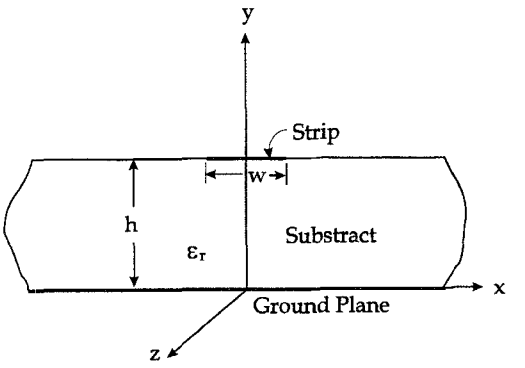

Fig. 2. The cross section of a microstrip configuration.

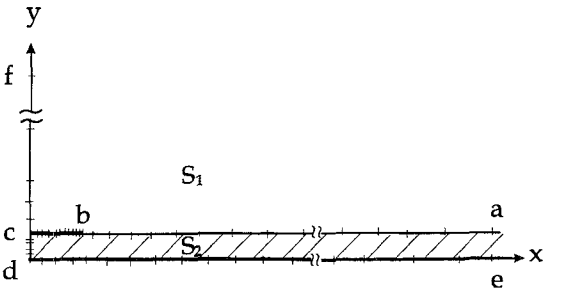

Fig. 3. Half cross section of a microstrip and the discretization on its boundaries.

Due to symmetry of the structure, we may place a magnetic (or electric) wall on the $x = 0$ plane to group propagation modes into two kinds. For example, the fundamental mode (first order mode) has magnetic wall on the $x = 0$ plane; whereas the second order mode has electric wall. Therefore, instead of Fig. 2, we consider the quarter space ($x \geq 0$, $y \geq 0$) as shown in Fig. 3 for simplicity. Boundary conditions, in this case, can be described as

$$\begin{cases} E_z, & \dfrac{\partial H_z}{\partial n} = 0, \quad \text{(on electric wall)} \\ \dfrac{\partial E_z}{\partial n}, & H_z = 0, \quad \text{(on magnetic wall)} \end{cases} \tag{9}$$

and, along the dielectric interface $\overline{ab}$ in Fig. 3 as

$$\begin{cases} \beta\dfrac{\partial H_z}{\partial x}\left(\dfrac{1}{k_2^a} - \dfrac{1}{k_d^2}\right) = w\varepsilon_0\left[\dfrac{1}{k_a^2}\dfrac{\partial E_z}{\partial y}\Big|_1 - \dfrac{\varepsilon_r}{k_d^2}\dfrac{\partial E_z}{\partial y}\Big|_2\right] \\ \beta\dfrac{\partial E_z}{\partial x}\left(\dfrac{1}{k_2^a} - \dfrac{1}{k_d^2}\right) = -w\,\mu_0\left[\dfrac{1}{k_a^2}\dfrac{\partial H_z}{\partial y}\Big|_1 - \dfrac{1}{k_d^2}\dfrac{\partial H_z}{\partial y}\Big|_2\right] \end{cases} \tag{10}$$

where the subscripts 1 and 2 in (10) stand for the free space and the dielectric space in Fig. 3, respectively [24].

IV. The Numerical Procedure

Since Fig. 3 is an open half structure, the boundary contour extends to infinity. Thus, for numerical calculation, we have to replace it with a finite contour. As shown in Fig. 3, the numbers of nodes discretized for boundary segments $\overline{ab}$, $\overline{bc}$, $\overline{cf}$, $\overline{cd}$, and $\overline{de}$ are N_1, N_2, N_3, N_4, and N_5, respectively. For each node, substituting ϕ_k, $[(\partial\phi)/(\partial n)]_k$ in (6) by $(E_z)k$,

$[(\partial E_z)/(\partial n)]_k$ and $(H_z)_k$, $[(\partial H_z)/\partial n)]_k$ in each region S_i, respectively, and applying the boundary condition (9), we obtain $2(N_1 + N_2 + N_3)$ homogeneous linear equations for the free space S_1 and $2(N_1+N_2+N_4+N_5)$ for the dielectric region S_2. These equations can be expressed as

$$[C^i]\begin{bmatrix} E_z \\ H_z \\ \dfrac{\partial E_z}{\partial n} \\ \dfrac{\partial H_z}{\partial n} \end{bmatrix} = 0; \quad i = 1, 2 \tag{11}$$

where 1 and 2 stand for regions S_1 and S_2, respectively. The orders of $[C^1]$ and $[C^2]$ are $2(N_1+N_2+N_3)\times(4N_1+2N_2+2N_3)$ and $2(N_1+N_2+N_4+N_5)\times(4N_1+2N_2+2N_4+2N_5)$. The number of columns in $[C^i]$ represents the number of unknowns in space S_i. In order to obtain the elements in $[C^i]$, the following formulas [23] are useful to compute the integration which passes through a singular point.

$$\begin{aligned}
&\int_0^l xK_0(kx)\,dx \approx \frac{l}{k}\left[\frac{1}{kl} - K_1(kl)\right] \\
&\int_0^l xH_0(kx)\,dx \approx \frac{l}{k}\left[-\frac{2i}{kl\pi} - H_1(kl)\right] \\
&\int_0^l K_0(kx)\,dx \approx l[\ln 2 - \ln(kl) - \gamma + 1] \\
&\int_0^l H_0(kx)\,dx \approx l + \frac{2il}{\pi}[\ln 2 - \ln(kl) - \gamma + 1]
\end{aligned} \tag{12}$$

where γ is the Euler–Maclaurin constant and l should be chosen to be small enough such that the above approximation is valid.

Furthermore, using Gaussian elimination method [25] to eliminate those variables which are not on the dielectric interface $\overline{ab}$, we can reduce the order of $[C^i]$ to $2N_1 \times 4N_1$. Combining the reduced $[C^1]$, $[C^2]$ and imposing boundary condition (9) to each node on $\overline{ab}$, one obtains

$$[D]\begin{bmatrix} E_z \\ H_z \\ \dfrac{\partial E_z}{\partial n} \\ \dfrac{\partial H_z}{\partial n} \end{bmatrix} = 0. \tag{13}$$

Since E_z, H_z, are continuous along interface $\overline{ab}$, there are $6N_1$ unknowns to solve and the final matrix $[D]$'s order is $6N_1 \times 6N_1$. Nontrivial solution exists only if $\det[D] = 0$. Note that elements D_{ij} in $[D]$ involve values of β and w. Under the condition of $\det[D] = 0$, we can find out that, for each frequency, there are several β's satisfied. Each β should be bounded by $1 \le \beta/k_0 \le \sqrt{\varepsilon_r}$ and corresponds to one propagation mode. Here k_0, the wave number in free space, is equal to $w\sqrt{\varepsilon_0\mu_0}$. From the frequency dependent β, one can obtain the dispersion relation and the effective dielectric constant ε_{eff} which is equal to $(\beta/k_0)^2$.

Since we discretize the finite boundary that approximates the infinite boundary, it is difficult to achieve the requirement $\det[D] = 0$. Therefore, instead, we try to find out local minima of $|\det[D]|$. Each ε_{eff} that gives a minimal $|\det[D]|$ would correspond to a propagation mode. In implementing the numerical procedure, the adaptive method is used to determine the range and the distribution of nodes on the boundaries. First, based on the electrostatic field distributions calculated using the analytical solution incorporated with electrode discretization technique [6], an initial discretizing configuration is established. As shown in Fig. 3, the initial truncation points are chosen at locations where the electrostatic field value decreases to 0.001 of the value at the center of stripline, i.e., point c in Fig. 3. For typical data presented in Fig. 4, the initial truncation points a, e, and f are found relative to other points by the relations $\overline{ca} = \overline{de} = 15\overline{cd}$, $cf = 10\overline{cd}$. At the chosen truncation points, the field value is set to zero. Using iteration by decent method[1] to search for the corresponding ε'_{eff} that gives minimal $|\det[D]|$ over all possible ε, and varying the position of each node, including the truncation points, we can obtain the ε_{eff} which is the stationary global minimum of $|\det[D]|$ among these ε'_{eff}. If this condition cannot be reached, new guess is tried. The order of iteration is $O(N_1 + N_3 + N_5)$, since the nodes on $\overline{bc}$, $\overline{cd}$ are fixed in this paper.

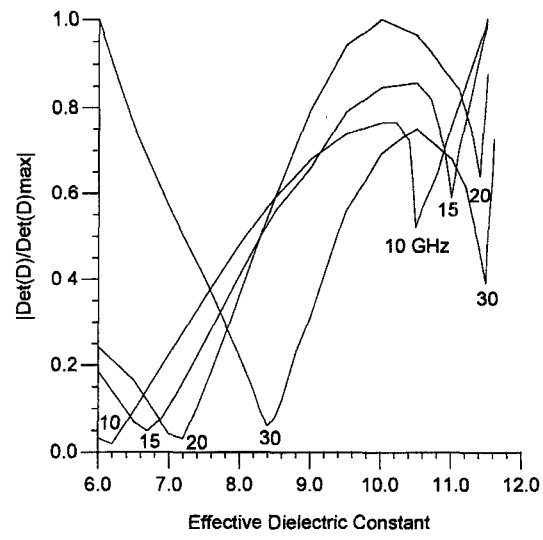

Fig. 4. Absolute value of determinant D versus effective dielectric constant with the magnetic wall on $x = 0$ plane ($h = 3.17$ mm, $w = 3.048$ mm, $\varepsilon_r = 11.7$, $N_t = 50$, $N_1 = 12$, $N_2 = 11$, $N_3 = 6$, $N_4 = 5$, and $N_5 = 16$).

V. Numerical Results

Based on the preceding procedure, a FORTRAN program has been implemented in workstation NCD 19C. The running time of a search of $\det[D]$ for the typical order ($N_t = 50$, $N_l = 12$) is 12 s. A microstrip shown in Fig. 2 with $h = 3.17$ mm, $w = 3.048$ mm, and $\varepsilon_r = 11.7$ is analyzed using the formulation developed above. This particular microstrip is chosen so that the calculated results can be compared with the reported values. Fig. 4 exhibits the $|\det[D]|$ versus the effective dielectric constant ε_{eff} with the magnetic wall on $x = 0$ plane for four frequencies. One curve is obtained

[1] We try both positive and negative direction to see which one gives decreasing $|\det[D]|$.

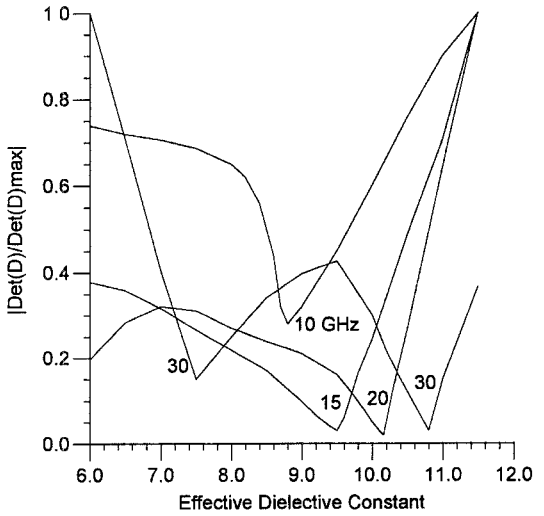

Fig. 5 Absolute value of determinant D versus effective dielectric constant with the electric wall on $x = 0$ plane ($h = 3.17$ mm, $w = 3.048$ mm, $\varepsilon_r = 11.7$, $N_t = 50$, $N_1 = 12$, $N_2 = 11$, $N_3 = 6$, $N_4 = 5$, and $N_5 = 16$).

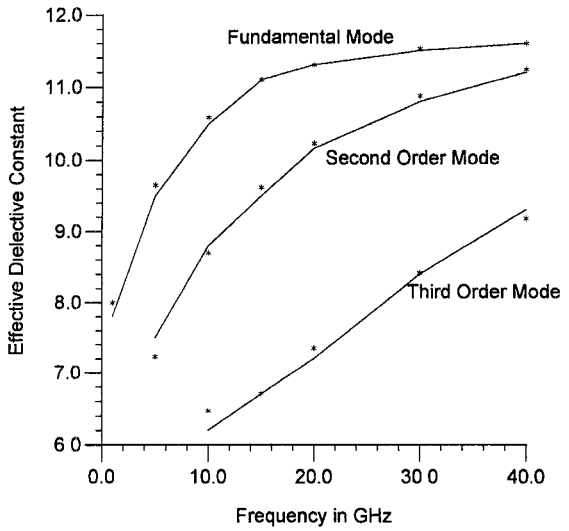

Fig. 6. Effective dielectric constant of the fundamental mode and higher order modes in the open microstrip line ($h = 3.17$ mm, $w = 3.048$ mm, $\varepsilon_r = 11.7$, $N_t = 50$, $N_1 = 12$, $N_2 = 11$, $N_3 = 6$, $N_4 = 5$, and $N_5 = 16$), Farrar and Adams [11].

for each frequency. There are two ε_{eff} values that give minimum values of $|\det[D]|$. The higher ε_{eff} corresponds to the fundamental mode; whereas the lower one corresponds to the third order mode. The dips for the fundamental mode are very sharp because they are close to c, that is the maximum possible ε_{eff}. Note that the width of these dips becomes wider at lower frequency, i.e., the accuracy of ε_{eff} becomes less for lower frequency.

Fig. 5 presents the $|\det[D]|$ with the electric wall on $x = 0$ plane. The curves for 10, 15, and 20 GHz have one minimum $|\det[D]|$ at ε_{eff} that belongs to the second order mode; whereas the curve for 30 GHz has two minima which correspond to the second and fourth order modes. The total number of nodes used in Figs. 4 and 5 is $N_t = 50$ and the number of nodes along interface $\overline{ab}$ is $N_1 = 12$. Fig. 6 displays the collection of these modes as compared to the

TABLE I
CALCULATED ε_{eff} OF THE SECOND ORDER MODE AT 5 GHz VERSUS THE TOTAL NUMBER OF NODES THE DISCREPANCY OF CALCULATED ε_{eff} FROM THE 7.176 VALUE THAT WAS REPORTED IN [10]

Division	N_t	N_l	ε_{eff}	Dis.
1	45	10	7.825	9%
2	50	12	7.452	3.8%
3	57	15	7.197	0.28%
4	65	18	7.178	0.03%

TABLE II
A COMPARISON ON THE CALCULATED ε_{eff} WITH OTHER METHODS A: FEM BY SHIH [16]; B: FEM BY LEE [15]; C: PRESENT METHOD

Methods	Node number	Order of [D]	Accuracy
A	81	162 x 162	10^{-4}
B	80	160 x 160	10^{-1}
C_1	50	72 x 72	10^{-1}
C_2	57	90 x 90	10^{-2}
C_3	65	108 x 108	10^{-3}

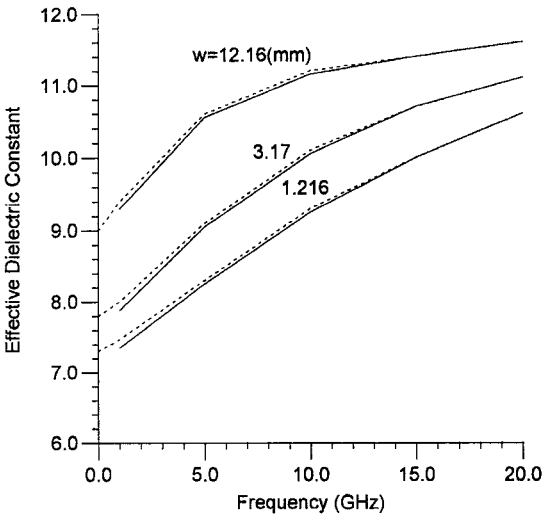

Fig. 7. Effective dielectric constant of fundamental modes ($h = 3.04$ mm, $\varepsilon_r = 11.7$, $w = 12.16, 3.17, 1.215$ mm Shih *et al.* [16] - - - : present method.

previous work analyzed by Farrar [11]. Results agree well for the fundamental mode; the agreement is less favorable for higher order modes at low frequency since it has broader and more varying field distribution. However, it can be improved greatly by increasing the number of nodes as shown in Table I. For example, by increasing the total number of nodes from 50 to 65, the discrepancy on the calculated ε_{eff} for the second order mode at 5 GHz from that reported in [10] can be reduced from 3.8 to 0.03%.

Fig. 7 provides the effective dielectric constants for the structure with various strip width $w = 12.16$, 3.17, and 1.215 mm in the same dielectric substrate with $\varepsilon_r = 11.7$ and height $h = 3.04$ mm. Our results agree with Shih *et al.*'s, results [16]. The deviation is less than 2%. A comparison with the available data of finite element methods is shown in Table II. Our method can reach 10^{-3} accuracy with the number of nodes increasing to 65.

After determining ε_{eff}, we can use (12) and Maxwell's equations to obtain field values on $\overline{ab}$. By way of this, surface

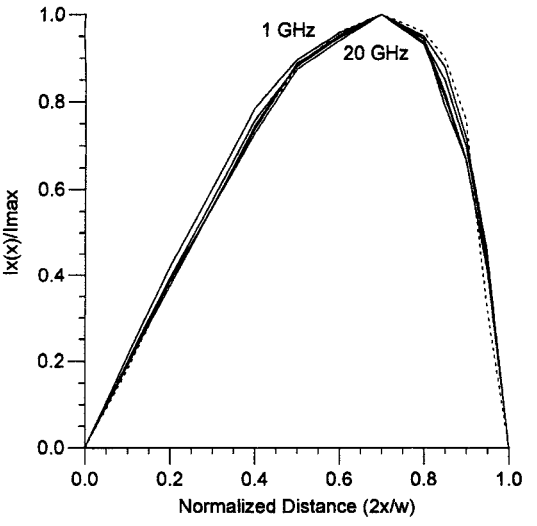

(a)

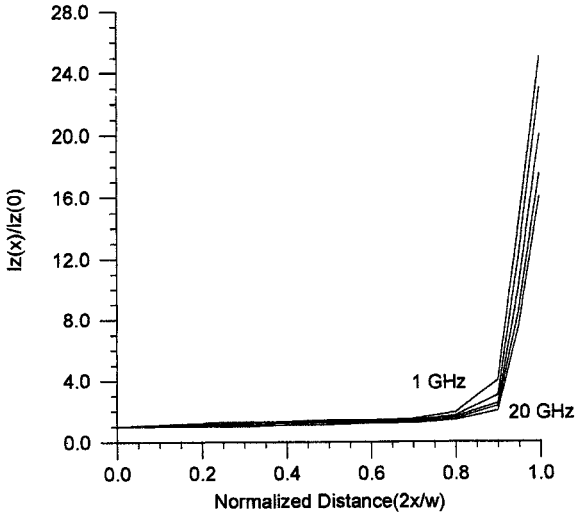

(b)

Fig. 8. Normalized current distribution of the fundamental mode versus normalized distance with frequency as a parameter. $h = 3.04$ mm, $\varepsilon_r = 11.7$, and frequency = 1, 5, 10, 15, and 20 GHz. (a) transverse current $I_x(x)$ and (b) longitudinal current $I_z(x)$, Shih *et al.* [16] - - - ; present method.

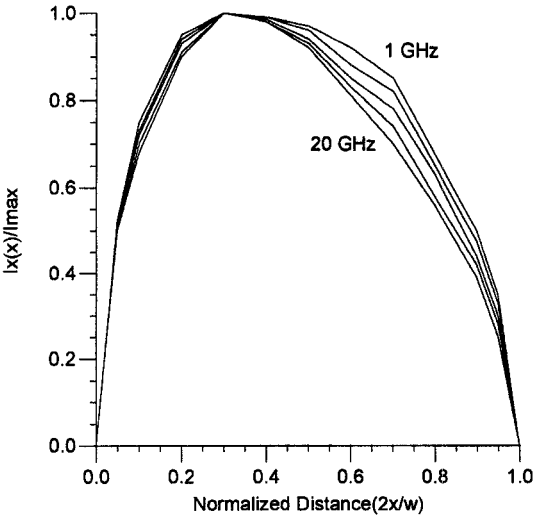

(a)

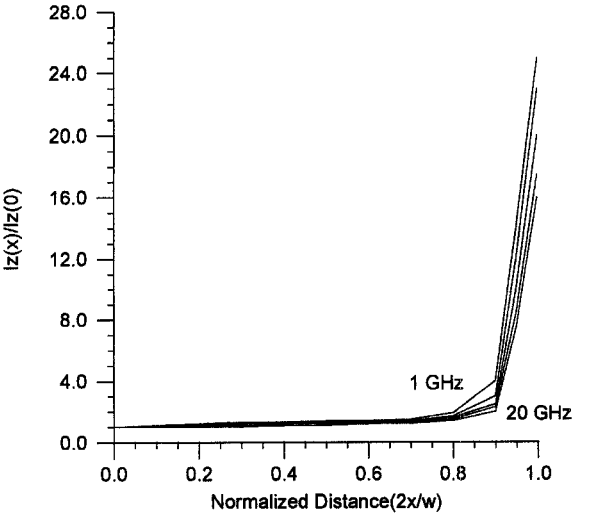

(b)

Fig. 9. Normalized current distribution of the second order mode versus normalized distance with frequency as a parameter. $h = 3.04$ mm, $\varepsilon_r = 11.7$ and frequency = 1, 5, 10, 15, and 20 GHz. (a) transverse current $I_x(x)$ and (b) longitudinal current $I_z(x)$.

current distributions I_x, and I_z, can be obtained from boundary conditions, i.e., $I_x = H_{z1} - H_{z2}$ and $I_z = H_{x2} - H_{x1}$. Fig. 8 displays the current distributions of $I_x(x)/I_{x\,\max}$ and $I_x(x)/I_z(0)$ for the fundamental mode. Fig. 9 shows the current distributions for the second order mode. Fig. 8 agrees well with Shih *et al.*'s results [16]. The current distribution I_x tends to concentrate more at the edge of the strip for the fundamental mode and toward the center for the second order mode as frequency becomes higher. However, they do not change much with frequency.

The method presented here can also be applied to coupled microstrip lines as shown in Fig. 10. Fig. 11 shows the computed effective dielectric constants of the even- and odd-modes versus frequency for various spacing between the two strips. The strip width, substrate height and dielectric constant are 0.6 mm, 0.64 mm, and 9.9, respectively. The discrepancy is within 5% compared with the results of Jansen [26]. The numbers of nodes in $\overline{ab}$ and $\overline{cd}$ are 10 and 8, respectively, and the total number of nodes is 75. The CPU time for each iteration of $\det[D]$ for the typical order ($N_t = 50$, $N_1 = 12$) is 12 s using NCD 19C workstation, as compared to 50 min for 1232 triangular elements using vector finite element method on the Standard Model P3 computer by Slade and Webb [27], and to 120 s for the first-order and 500 s for the second-order modes using the spectral-domain method on CDC G-20 computer by Itoh and Mittra [10].

VI. Conclusion

A full-wave analysis of open structure microstrip problem using the BEM has been presented. This method, in numerical calculation, is characterized by the reduction of memory size without resorting to intricate mathematical skills. Numerical results of the effective dielectric constants for the fundamental

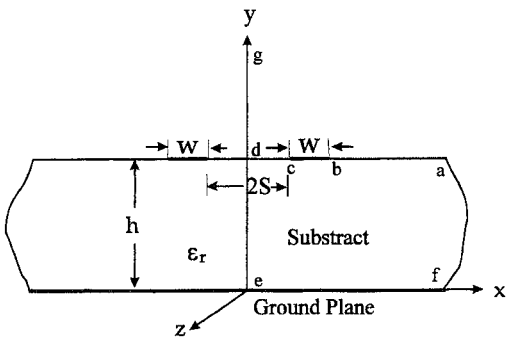

Fig. 10. Cross section of coupled microstrip lines.

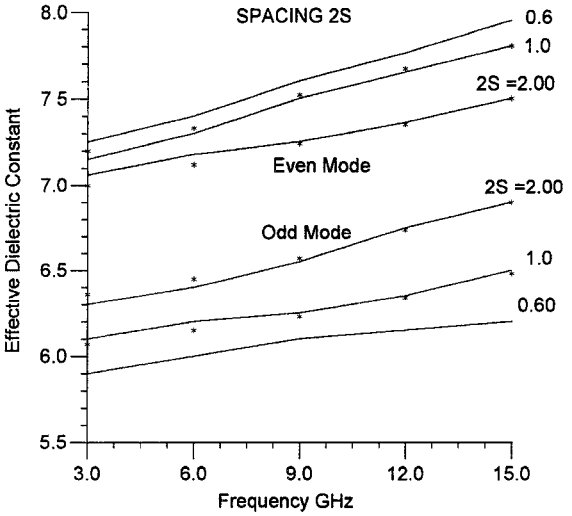

Fig. 11. Effective dielectric constant of the even- and odd-modes propagating along coupled microstrip lines with varying spacing. $w = 0.6$ mm, $h = 0.64$ mm, and $\varepsilon_r = 9.9$, Jansen [26] ***; present method.

and higher order modes have been obtained. Longitudinal and transverse current distributions are also shown. In each case the results are in good agreement with published results. Besides regular microstrip line, coupled microstrip lines have also been analyzed.

This method is rather general and thus can be extended to other more complicated structures, such as microstrips with multilayered substrate, microstrips of finite metallization thickness, and the coplanar microstrip.

REFERENCES

[1] H. A. Wheeler, "Transmission line properties of parallel strip separated by a dielectric sheet," *IEEE Trans. Microwave Theory Tech.*, vol. MTT-13, pp. 172–185, 1965.

[2] R. F. Harrington, *Field Computation by Moment Methods.* New York: MacMillan, 1968; Melbourne, FL: Krieger, reprinted 1982.

[3] E. Yamashita and R. Mittra, "Variational method for the analysis of microstrip lines," *IEEE Trans. Microwave Theory Tech.*, vol. MTT-16, pp. 251–256, 1968.

[4] M. V. Schneider, "Microstrip lines for microwave integrated circuits," *Bell Syst. Tech. J.*, vol. 48, pp. 1421–1444, 1969.

[5] C. E. Smith and R. S. Chang, "Microstrip transmission line with finite-width dielectric," *IEEE Trans. Microwave Theory Tech.*, vol. MTT-28, pp. 90–94, 1980.

[6] C. C. Lee and D. H. Chien, "Electrostatics and thermostatics: A connection between electrical and mechanical engineering," *Int. J. Engineering Education*, vol. 10, pp. 434–449, 1994.

[7] M. Kobayashi,"Longitudinal and transverse current distributions on microstriplines and their closed-form expression," *IEEE Trans. Microwave Theory Tech.*, vol. MTT-33, pp. 784–788, Sept. 1985.

[8] D G. Corr and J. B. Davies, "Computer analysis of fundamental and higher order modes in single and coupled microstrip," *IEEE Trans. Microwave Theory Tech.*, vol. MTT-30, no. 10, pp. 669–678, Oct. 1972.

[9] E. Schwig and W. B. Bridges, "Computer analysis of dielectric waveguides: A finite difference method," *IEEE Trans. Microwave Theory Tech.*, vol. MTT-32, pp. 531–541, May 1984.

[10] T. Itoh and R. Mitta, "Spectral domain approach for calculating the dispersion characteristics of microstrip lines," *IEEE Trans. Microwave Theory Tech.*, vol. MTT-21, pp. 496–499, July 1973.

[11] A. Farrar and A. T. Adams, "Computation of propagation constants for the fundamental and higher order modes in microstrip," *IEEE Trans. Microwave Theory Tech.*, vol. MTT-24, pp. 456–460, July 1976.

[12] M. Kobayashi and F. Ando, "Dispersion characteristics of open microstrip line," *IEEE Trans. Microwave Theory Tech.*, vol. MTT-35, no. 2, pp. 101–105, Feb. 1987.

[13] P. Daly, "Hybrid-mode analysis of microstrip by finite-element methods," *IEEE Trans. Microwave Theory Tech.*, vol. MTT-19, pp. 19–25, Jan. 1971.

[14] B. M. A. Rahman and J. B. Davies, "Finite-element analysis of optical and microwave waveguide problems," *IEEE Trans. Microwave Theory Tech.*, vol. MTT-32, pp. 20–28, Jan. 1984.

[15] J. F. Lee, D.-K. Sun, and Z. J. Cendes, "Full-wave analysis of dielectric waveguides using tangential vector finite elements," *IEEE Trans. Microwave Theory Tech.*, vol. 39, no. 8, pp. 1262–1271, Aug. 1991.

[16] C. Shih, R. B. Wu, S. K. Jeng, and C. H. Chen, "A full-wave analysis of microstrip lines by variational conformal mapping technique," *IEEE Trans. Microwave Theory Tech.*, vol. 36, no. 3, pp. 576–581, Mar. 1988.

[17] C. A. Brebbia, *The Boundary Element Method for Engineers.* London: Pentech Press, 1978.

[18] S. Kagami and I. Fukai, "Application of boundary-element method to electromagnetic field problems," *IEEE Trans. Microwave Theory Tech.*, vol. 32, no. 4, pp. 455–461, Apr. 1984.

[19] M. Koshiba and M. Suzuki, "Application of boundary element method to waveguide discontinuities," *IEEE Trans. Microwave Theory Tech.*, vol. MTT-34, no. 2, pp. 301–307, Feb. 1986.

[20] B. Song and J. Fu, "Application of modified indirect boundary-element method to electromagnetic problems," *IEEE Trans. Microwave Theory Tech.*, vol. 42, no. 4, pp. 729–731, Apr. 1994.

[21] K. Yashiro, M. Miyazaki, and S. Ohkawa, "Boundary element methods approach to magnetostatic wave problems," *IEEE Trans. Microwave Theory Tech.*, vol. MTT-33, no. 3, pp. 248–252, Mar. 1985.

[22] T. N. Chang and Y. T. Lin, "Quasistatic analysis of shielded microstripline by a modified boundary element method," *IEEE Trans. Microwave Theory Tech.*, vol. 41, no. 4, pp. 729–731, Apr. 1993.

[23] G. Arfken, *Mathematical Methods for Physicists.* Orlando: Academic Press, 1985.

[24] D. M. Pozar, *Microwave Engineering.* MA: Addison-Wesley Company, 1990.

[25] M. J. Moron, *Numerical Analysis: A Practical Approach.* New York: Collier Macmillan, 1987.

[26] R. H. Jansen, "High-speed computation of single and coupled microstrip parameters including dispersion, high-order modes, loss and finite strip thickness," *IEEE Trans. Microwave Theory Tech.*, vol. MTT-26, no. 2, pp. 75–82, Feb. 1978.

[27] G. W. Slade and K. J. Webb, "Computation of characteristic impedance for multiple microstrip transmission lines using a vector finite element method," *IEEE Trans. Microwave Theory Tech.*, vol. 1, no. 1, pp. 34–40, Jan. 1992.

Shih-Yuan Lin was born in Taiwan. He received the B.S. degree in physics from National Tsing Hua University, Taiwan, and the M.S. degree in electrical engineering from National Taiwan University, in 1987 and 1992, respectively.

He taught at Fu-Shing Junior College, Taiwan, for a year. In 1993, he joined the Electrical and Computer Engineering Department at the University of California, Irvine, as a graduate student. He is currently working toward the Ph.D. degree. His research interests include electromagnetic theory, wave propagation, and numerical techniques.

Chin C. Lee (S'74–M'79–SM'89) was born in Taiwan in 1948. He received the B.E. and M.S. degrees in electronics from the National Chiao-Tung University, Hsinchu, Taiwan, in 1970 and 1973, respectively, and the Ph.D. degree in electrical engineering from Carnegie-Mellon University, Pittsburgh, PA, in 1979.

From 1979 to 1980, he was a Research Associate with the Electrical Engineering Department of Carnegie-Mellon University. From 1980 to 1983, he was with the Electrical Engineering Department of the University of California, Irvine, as a Research Specialist. In 1984, he joined the same department as an Assistant Professor and became Professor of Electrical and Computer Engineering in July 1994. He served as the Graduate Advisor of Electrical and Computer Engineering at UCI from 1990/91 to 93/94. His research interests include electronic packaging technology, thermal analysis and design of electronic devices, integrated optics, optoelectronics, electromagnetic theory, acoustic microscopy and acoustics. He has co-authored three book chapters and more than 100 papers in the subject areas mentioned above.

Dr. Lee is a member of the International Society for Boundary Elements and Tau Beta Pi. He is an associate editor of IEEE TRANSACTIONS ON COMPONENTS, PACKAGING, AND MANUFACTURING TECHNOLOGY.